Study of weakly damped superconducting quantum interference devices operated in different bias modes in presence of external shunt resistance

Jia Zeng, Yi Zhang, Michael Mück, Hans-Joachim Krause, Alex I. Braginski, Xiangyan Kong, Xiaoming Xie, Andreas Offenhäusser, and Mianheng Jiang

Citation: Applied Physics Letters **103**, 122605 (2013); doi: 10.1063/1.4821852
View online: http://dx.doi.org/10.1063/1.4821852
View Table of Contents: http://scitation.aip.org/content/aip/journal/apl/103/12?ver=pdfcov
Published by the AIP Publishing

APPLIED PHYSICS LETTERS **103**, 122605 (2013)

Study of weakly damped superconducting quantum interference devices operated in different bias modes in presence of external shunt resistance

Jia Zeng,[1,2,3,4] Yi Zhang,[2,3,a)] Michael Mück,[5] Hans-Joachim Krause,[2,3] Alex I. Braginski,[2] Xiangyan Kong,[1,3] Xiaoming Xie,[1,3] Andreas Offenhäusser,[2,3] and Mianheng Jiang[1,3]
[1]*State Key Laboratory of Functional Materials for Informatics, Shanghai Institute of Microsystem and Information Technology (SIMIT), Chinese Academy of Sciences (CAS), Shanghai 200050, China*
[2]*Peter Grünberg Institute (PGI-8), Forschungszentrum Jülich (FZJ), D-52425 Jülich, Germany*
[3]*Joint Research Laboratory on Superconductivity and Bioelectronics, Collaboration between CAS-Shanghai, Shanghai 200050, People's Republic of China and FZJ, D-52425 Jülich Germany*
[4]*University of Chinese Academy of Sciences, Beijing 100049, China*
[5]*ez SQUID, Herborner Strasse 9, D-35764 Sinn, Germany*

(Received 30 July 2013; accepted 4 September 2013; published online 20 September 2013)

We experimentally studied weakly damped superconducting quantum interference devices (SQUIDs) shunted by an external resistor R_s and operated in either current- or voltage-bias mode. The SQUID parameters, such as the flux-to-voltage transfer coefficient $\partial V/\partial\Phi$ and the dynamic resistance R_d, are reduced due to R_s, while the SQUID intrinsic noise remains unchanged. The reduced parameters can be enhanced again by using voltage feedback circuitry. Furthermore, R_s can be used to damp the SQUID in order to avoid the appearance of hysteresis or oscillation in SQUID characteristics. SQUID shunted by small R_s is always operated in mixed-bias mode. © *2013 AIP Publishing LLC*. [http://dx.doi.org/10.1063/1.4821852]

Generally, superconducting quantum interference devices (SQUIDs) are operated either in the current-bias (I_b) mode or the voltage-bias (V_b) mode. With respect to noise, there is no difference between the two bias modes.[1]

In the current-bias mode, the current flowing through SQUID should be kept constant when the external flux, $\Delta\Phi_a$, changes. However, the SQUID is shunted by the readout circuit representing an impedance Z_s or resistor R_s. The primary winding of the transformer in the flux modulation scheme[2] or additional feedback circuitries such as additional positive feedback (APF)[3] are impedance shunts which influence the SQUID bias current. When $|Z_s|$ or $R_s \gg R_d$ (SQUID dynamic resistance) is not fulfilled, the SQUID bias current varies with varying R_d, once the external flux, $\Delta\Phi_a$, is applied. Although the total current flowing through both the SQUID and the shunt remains constant, the SQUID is essentially biased in mixed-bias mode. When $R_s \ll R_d$ is fulfilled, the voltage across SQUID and R_s is quasi constant and the device is voltage-biased.[4] Another possibility to realize the voltage-bias mode is to use a current-to-voltage converter.[5,6] When the voltage source internal resistance R_{in} is comparable to the value of R_s shunting R_d, the voltage across the externally shunted SQUID changes with $\Delta\Phi_a$, i.e., the SQUID is again operated in mixed-bias mode.

Traditionally, most SQUIDs are operated in the current-bias mode.[7] Recently, we studied the performance of voltage-biased SQUIDs with different Steward-McCumber parameters, β_c.[8,9] Different β_c values were obtained by varying the junction internal shunt resistors R_J, while keeping the junction capacitance and the critical current unchanged. It was found that the SQUID intrinsic noise $\delta\Phi_s$, its flux-to-voltage transfer coefficient $\partial V/\partial\Phi$, and the dynamic resistance R_d increase with increasing junction's R_J.[10]

Our objective in this work has been to study the behavior of weakly damped SQUIDs shunted by an additional external resistance R_s and to compare their performance when in different (nominally current or voltage) bias modes. Parameters of the original SQUID with and without external shunt were recorded for two values of $\beta_c > 1$ or $\gg 1$, and noise analysis was performed. The combination of the SQUID and the external shunt resistor R_s can be regarded as a device in itself, an externally shunted SQUID.

We constructed a SQUID readout electronics which can be switched between current- and voltage-bias mode. Its equivalent circuit is schematically shown in Figure 1. Note, each SQUID with its output electronics is represented by a flux-to-voltage ($\partial V/\partial\Phi$) converter with the nonlinear resistor R_d in series. When the switch K is in position "1," the externally shunted SQUID is current-biased and the voltage signal is read out by a voltmeter V. In the K position "2," the device is in voltage-bias mode where the current signal flowing through the SQUID is read out by an ammeter A. In both bias modes, the same ultra-low noise preamplifier consisting of 6 parallel-connected bipolar transistors (AD-SSM2220) with measured voltage noise of $V_n \approx 0.37$ nV/$\sqrt{\text{Hz}}$ ($f > 2$ Hz) was connected to the externally shunted SQUID in the direct readout scheme. It yielded a high sensitivity either as voltmeter V or ammeter A. The same two SQUIDs and the same preamplifier were used in this work to assure full comparability in both bias modes.

Two planar niobium-SQUID magnetometers, one with $\beta_c \approx 3$ and another with $\beta_c \gg 1$, but otherwise nominally similar, were used to study the externally shunted SQUID performance in different bias modes. The field-to-flux transfer coefficient $\partial B/\partial\Phi$ of both SQUID magnetometers was 1.5 nT/Φ_0 with a pick-up-loop size of 5×5 mm^2 and a

a)Author to whom correspondence should be addressed. Electronic mail: y.zhang@fz-juelich.de

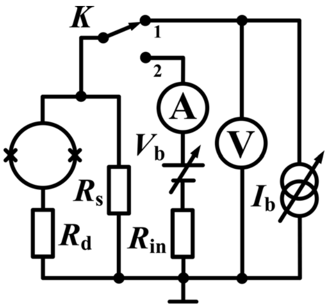

FIG. 1. Equivalent circuit of the externally shunted SQUID with both current- and voltage-sources, voltmeter V, and ammeter A. The bias mode can be chosen by switch K. The externally shunted SQUID device consists of the SQUID itself with its dynamic resistance R_d in series and the shunt resistance R_s.

SQUID inductance of $L_s = 350$ pH. The chip layout is shown in Ref. 8. The SQUID under study was placed in a niobium shielding tube to perform the noise measurements in flux-locked-loop (FLL).

The weakly damped SQUID #1 with $\beta_c \approx 3$ leads to a large flux-to-voltage transfer coefficient $\partial V/\partial\Phi \approx 490\,\mu V/\Phi_0$, thus reducing the preamplifier noise contribution to $\delta\Phi_{preamp} = V_n/(\partial V/\partial\Phi) \approx 0.8\,\mu\Phi_0/\sqrt{\text{Hz}}$. The measured SQUID system noise $\delta\Phi = [\delta\Phi_s{}^2 + \delta\Phi_{preamp}{}^2]^{1/2} \approx 3.5\,\mu\Phi_0/\sqrt{\text{Hz}}$ is clearly dominated by the SQUID intrinsic flux noise $\delta\Phi_s$, i.e., $\delta\Phi \approx \delta\Phi_s$. We shunted SQUID #1 with three different resistors R_s to observe the performance changes. The measured parameters of SQUID #1 with and without ($R_s = \infty$) external shunts are listed in Table I.

In the voltage-bias mode, the shunt R_s did not significantly influence the current swing $I_{swing} \approx 3\,\mu$A and the flux-to-current transfer coefficient $\partial i/\partial\Phi \approx 10\,\mu A/\Phi_0$, independent of the R_s value. However, the dynamic SQUID resistance of any shunted device was reduced, and so was the transfer coefficient $\partial V/\partial\Phi$ obtained as the product $(\partial i/\partial\Phi) \times R_d$, because R_s // R_d, For the same reason, in the current-bias mode, the voltage swing V_{swing}, $\partial V/\partial\Phi$, and R_d of the externally shunted SQUID decreased with decreasing R_s. It is very interesting that the value of $\partial V/\partial\Phi$, but not the voltage swing V_{swing}, was proportional to the ratio of $R_s/(R_s + R_d)$.

The measured system noise $\delta\Phi$ of the externally shunted SQUID consists of $\delta\Phi_s$, $\delta\Phi_{preamp}$ and the noise contribution of R_s, $\delta\Phi_R$, i.e., $\delta\Phi = [\delta\Phi_s{}^2 + \delta\Phi_{preamp}{}^2 + \delta\Phi_R{}^2]^{1/2}$. However, $\delta\Phi_R = (\sqrt{4k_BT/R_s} \times R_d)/(\partial V/\partial\Phi) < 1\,\mu\Phi_0/\sqrt{\text{Hz}}$ (k_B denotes the Boltzmann constant and T the temperature) can be neglected, because $\delta\Phi_s \approx 3.5\,\mu\Phi_0/\sqrt{\text{Hz}}$ is much higher than $\delta\Phi_R$. Note that R_s produces a negligible noise contribution only if the SQUID is symmetric with respect to its bias leads. Due to a circulating noise current generated by R_s through the two arms of SQUID, any non-symmetry in the SQUID will lead to an additional flux noise in the SQUID-loop. As could be expected, $\delta\Phi_s$ remained unchanged with or without R_s in both bias modes, while $\delta\Phi_{preamp}$ monotonously increased with decreasing R_s due to the decrease of $\partial V/\partial\Phi$. At $R_s = 5\,\Omega$, $\delta\Phi_{preamp} \approx 6.7\,\mu\Phi_0/\sqrt{\text{Hz}}$ dominated $\delta\Phi$ in both bias modes. Indeed, $\delta\Phi_s$ is an intrinsic SQUID property which should not be affected by external circuitry, although other SQUID parameters, e.g., $\partial V/\partial\Phi$ and R_d, are affected by R_s. Table I shows that $\delta\Phi_s$ and $\delta\Phi_{preamp}$ do not depend on the bias mode.

Figure 2(a) and its inset show I-V characteristics of SQUID #1 with and without $R_s = 5\,\Omega$ at integer and half integer flux quantum of applied flux. Shunt R_s increases the slope of I-V characteristics, i.e., decreases the effective dynamic resistance R_d. In the current-bias mode, the voltage swing V_{swing} is thus significantly reduced while I_{swing} remains unaffected. Figure 2(b) shows V-Φ and I-Φ traces when $R_s = \infty$; their amplitudes reflect V_{swing} and I_{swing}. Due to the large β_c, the V-Φ characteristic is close to a square wave,[10] thus leading to a large $\partial V/\partial\Phi \approx 490\,\mu V/\Phi_0$. In the voltage-bias mode, the I-Φ characteristic looks like a triangular wave and $\partial i/\partial\Phi \approx 10\,\mu A/\Phi_0$ was reached. The working points, W, for noise measurements with FLL are marked. In Figure 3(c), plot I is the measured SQUID system noise spectrum when $R_s = \infty$, with $\delta\Phi \approx \delta\Phi_s = 3.5\,\mu\Phi_0/\sqrt{\text{Hz}}$ in the white noise range for both bias modes.

We used the on-chip voltage feedback circuitry to increase $\partial V/\partial\Phi$ and R_d of the externally shunted SQUID

TABLE I. Measured parameters of SQUID #1 ($\beta_c \approx 3$) in both bias modes for different external shunts R_s.

R_s	[Ω]	5	5	15	15	30	30	∞	∞
Bias mode		I_b	V_b	I_b	V_b	I_b	V_b	I_b	V_b
V_{swing}[a]	[μV]	14	/	32	/	44	/	60	/
I_{swing}[a]	[μA]	/	3.2	/	3.1	/	3.2	/	2.9
$\partial V/\partial\Phi$[b]	[$\mu V/\Phi_0$]	55	55[g]	125	128[g]	225	242[g]	490	490[g]
$\partial i/\partial\Phi$[b]	[$\mu A/\Phi_0$]	/	11	/	10	/	11	/	9.8
R_d[c]	[Ω]	4	5	11.4	12.8	20	22	50	50
$\delta\Phi$[d]	[$\mu\Phi_0/\sqrt{\text{Hz}}$]	7.6	7.5	4.7	4.6	3.9	3.9	3.6	3.6
$\delta\Phi_{preamp}$[e]	[$\mu\Phi_0/\sqrt{\text{Hz}}$]	6.7	6.7	3	2.9	1.6	1.5	0.75	0.76
$\delta\Phi_s$[f]	[$\mu\Phi_0/\sqrt{\text{Hz}}$]	3.6	3.4	3.6	3.6	3.5	3.6	3.5	3.5

[a]measured from the $V(I)$-Φ curve.
[b]derived from the $V(I)$-Φ curve at the working point.
[c]derived from the I-V characteristics.
[d]measured SQUID system noise.
[e]estimated by $\delta\Phi_{preamp} = V_n/(\partial V/\partial\Phi)$.
[f]$\delta\Phi_s = (\delta\Phi^2 - \delta\Phi_{preamp}{}^2)^{1/2}$.
[g]obtained by multiplying $(\partial i/\partial\Phi) \times R_d$. Note that the connection between the SQUID (or externally shunted SQUID) and the preamplifier was the same in either bias mode.

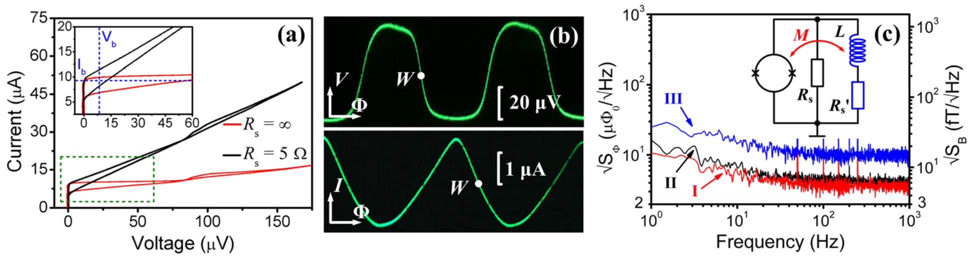

FIG. 2. (a) *I-V* characteristics of SQUID #1 with and without $R_s = 5\ \Omega$ at integer and half integer flux quantum. The inset enlarges the working region. (b) *V*-Φ (upper) and *I*-Φ (lower) characteristics of the employed SQUID #1 without R_s. (c) Flux noise spectrum $\sqrt{S_\Phi}$ measurements: plot I for the unshunted SQUID #1 and plot II when the externally shunted SQUID is shunted by the voltage feedback circuitry shown in the inset. Here, $M = 0.76$ nH and $R'_s = 20\ \Omega$. Plot III shows the spectrum of externally shunted SQUID #2 with $R_s = 15\ \Omega$. The right ordinate gives the field resolution $\sqrt{S_B}$.

with $R_s = 5\,\Omega$. It functions as APF[3] when the SQUID is current-biased and as noise cancellation (NC)[5] with voltage bias. The circuitry consisting of a coil L and a resistor R'_s shunts this externally shunted SQUID. The equivalent circuit of the feedback is shown in the inset of Figure 2(c). R'_s is chosen to be $M \times (\partial V/\partial \Phi) \approx 20\,\Omega$, where M is the mutual inductance between the SQUID loop and L. Figure 3(a) shows *V*-Φ characteristics with APF (upper trace) and *I*-Φ characteristics with NC (lower trace). With APF, the working point W was set on the steep slope with $\partial V/\partial \Phi \approx 200\,\mu V/\Phi_0$, thus reducing $\delta\Phi_{preamp}$ from $6.7\,\mu\Phi_0/\sqrt{\text{Hz}}$ to $1.9\,\mu\Phi_0/\sqrt{\text{Hz}}$. The NC scheme increased R_d from $5\,\Omega$ up to $20\,\Omega$ at W, thus increasing $\partial V/\partial \Phi$ from $55\,\mu V/\Phi_0$ (see Table I) up to $200\,\mu V/\Phi_0$. The value $\delta\Phi \approx 4\,\mu\Phi_0/\sqrt{\text{Hz}}$ (white noise range) with either APF or NC is obtained from plot II of Figure 2(c), which rather close to plot I. The main difference between APF and NC is the linear flux range of *V*-Φ and *I*-Φ characteristics. Their derivatives, $(\partial V/\partial \Phi)$ *vs.* Φ_a (upper trace) and $(\partial i/\partial \Phi)$ *vs.* Φ_a (lower trace), are displayed in Figure 3(b). In APF (current bias), W set on a narrow peak of $\partial V/\partial \Phi$ may lead to instability, whereas there is a broader linear flux range around W in NC (voltage bias).

For the underdamped SQUID #2 with $\beta_c \gg 1$, a hysteretic *V*-Φ characteristic in the current-bias mode (a) and oscillating *I*-Φ characteristic in the voltage-bias mode (b) are shown in Figure 4. When SQUID #2 was shunted with $R_s < 20\,\Omega$, the hysteresis and the oscillation disappeared as illustrated by traces (c) and (d). The performance of the externally shunted SQUID # 2 with $R_s = 5\,\Omega$ was almost the same in both bias modes. The voltage source internal resistance $R_{in} \approx 0.5 \sim 1\,\Omega$ was insufficiently lower than $R_d = 5\,\Omega$, so that the SQUID operated in mixed-bias mode.

The measured parameters of the externally shunted SQUID #2 with different R_s in the current-bias mode are listed in Table II. The system noise $\delta\Phi$ is close to the intrinsic noise of $\delta\Phi_s \approx 10\,\mu\Phi_0/\sqrt{\text{Hz}}$ at $R_s \geq 15\,\Omega$. The spectrum when $R_s = 15\,\Omega$ is the plot III in Figure 2(c). As can be inferred from Table I, the dynamic resistance R_d should be smaller than the external shunt R_s. However, for SQUID #2 with $R_s = 20\,\Omega$, $R_d > R_s$. The SQUID dynamic resistance is then negative as discussed in Ref. 11. The negative dynamic resistance leads to the instability of the readout circuit. The disappearance of the hysteresis (c) and the oscillation (d) meant that R_s damps the negative dynamic resistance, but does not change the intrinsic property of SQUID#2.

In conclusion, the added external shunt R_s changes the values of original SQUID parameters, such as $\partial V/\partial \Phi$ and

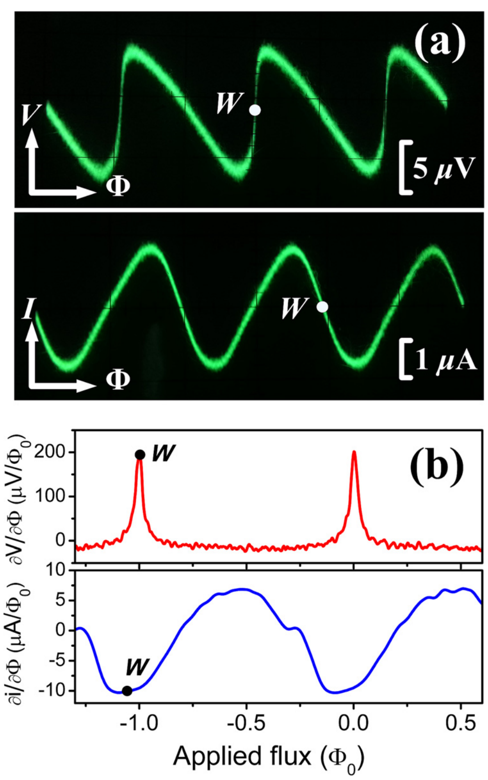

FIG. 3. (a) *V*-Φ and *I*-Φ characteristics of the externally shunted SQUID #1 ($R_s = 5\ \Omega$) with APF (upper trace) and NC (lower trace). (b) Derivatives $(\partial V/\partial \Phi)$ vs. Φ_a and $(\partial i/\partial \Phi)$ vs. Φ_a.

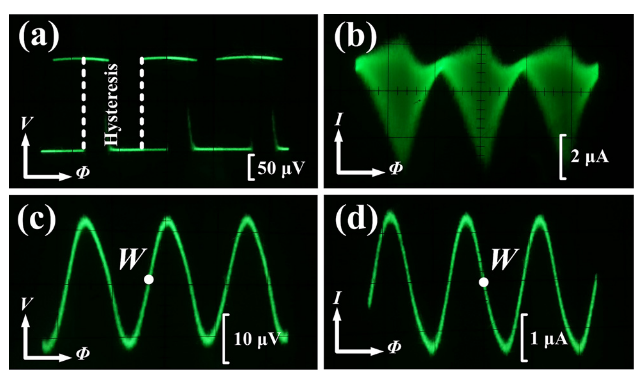

FIG. 4. Transfer characteristics of SQUID #2 with $\beta_c \gg 1$ at different bias modes; *V*-Φ characteristics in current-bias mode without shunt (a) and with external shunt $R_s = 5\ \Omega$ (c); *I*-Φ characteristics in voltage-bias mode without shunt (b) and with external shunt $R_s = 5\ \Omega$ (d).

TABLE II. Parameter measurements of SQUID #2 with different external shunts R_s in current-bias mode.

R_s	[Ω]	5	10	15	20
R_d	[Ω]	5	10	15	25
$\partial V/\partial\Phi$	[μV/Φ_0]	50	80	120	160
$\delta\Phi$	[$\mu\Phi_0/\sqrt{\text{Hz}}$]	12	11	10	10
$\delta\Phi_{preamp}$	[$\mu\Phi_0/\sqrt{\text{Hz}}$]	7.4	4.6	3	2.3
$\delta\Phi_s$	[$\mu\Phi_0/\sqrt{\text{Hz}}$]	9.4	10	9.5	9.7

R_d, while the intrinsic noise remains unaffected, because it is independent of any external circuitry and bias modes. In contrast, the junction internal shunt R_J affects intrinsic noise. Additional R_s can also suppress hysteresis or oscillation in SQUIDs with $\beta_c \gg 1$. Strictly speaking, the externally shunted SQUID is always operated in the mixed-bias mode, where one can read out the SQUID either via the voltage or current signal. The mixed-bias mode reduces the value of $\partial V/\partial\Phi$, thus increasing the contribution of preamplifier noise. In demonstrating the functions of APF and NC, we pointed out the different linear flux ranges of the two. In this respect, NC offers superior performance. The study of the externally shunted SQUIDs is meaningful for understanding the SQUID bias modes.

This work was supported by the "Strategic Priority Research Program (B)" of the Chinese Academy of Sciences (Grant No: XDB04010100).

[1]D. Drung and M. Mück, *in The SQUID Handbook*, edited by J. Clarke and A. I. Braginski (Wiley-VCH, Weinheim, 2004), Vol. I, pp. 127–170.
[2]R. L. Forgacs and A. Warnick, Rev. Sci. Instrum. **38**, 214 (1967).
[3]D. Drung, R. Cantor, M. Peters, H. J. Scheer, and H. Koch, Appl. Phys. Lett. **57**, 406–408 (1990).
[4]F. C. Wellstood, C. Urbina, and J. Clarke, Appl. Phys. Lett. **50**, 772 (1987).
[5]H. Seppä, A. Ahonen, J. Knuutila, J. Simola, and V. Vilkman, IEEE Trans. Magn. **27**, 2488–2490 (1991).
[6]X. Xie, Y. Zhang, H. Wang, Y. Wang, M. Mück, H. Dong, H.-J. Krause, A. I. Braginski, A. Offenhäusser, and M. Jiang, Supercond. Sci. Technol. **23**, 065016 (2010).
[7]J. Clarke, W. M. Goubau, and M. B. Ketchen, J. Low Temp. Phys. **25**, 99–144 (1976).
[8]Y. Zhang, C. Liu, M. Schmelz, H.-J. Krause, A. I. Braginski, R. Stolz, X. Xie, H.-G. Meyer, A. Offenhäusser, and M. Jiang, Supercond. Sci. Technol. **25**, 125007 (2012).
[9]C. Liu, Y. Zhang, M. Mück, H.-J. Krause, A. I. Braginski, X. Xie, A. Offenhäusser, and M. Jiang, Appl. Phys. Lett. **101**, 222602 (2012).
[10]J. Zeng, Y. Zhang, M. Mück, H.-J. Krause, A. I. Braginski, X. Kong, X. Xie, A. Offenhäusser, and M. Jiang, Appl. Phys. Lett. **103**, 042601 (2013).
[11]Y. Taur and P. L. Richards, J. Appl. Phys. **46**, 1793 (1975).